Identification of a MIMO state space model of an F/A-18 aircraft using a subspace method

S. De Jesus-Mota, M. Nadeau Beaulieu and R. M. Botez
ruxandra@gpa.etsmtl.ca
École de technologie supérieure
Department of Automated Production Engineering Laboratory of Research in Active Controls, Aeroservoelasticity and Avionics
Montréal, Québec
Canada

ABSTRACT

The aim of this paper is to determine the mathematical relationship (model) between control deflections and structural deflections of the F/A-18 modified aircraft in the active aeroelastic wing technology program. Five sets of signals from flight flutter tests corresponding to the excited sources were measured by NASA Dryden Flight Research Center. These excitation inputs are: differential ailerons, collective ailerons, collective stabilisers, differential stabilisers, and rudders. The signals to be used by the model are of two types: control deflection time histories and corresponding structural deflections on the wing and trailing-edge flaps. We choose to use the subspace identification method based on reconstructing the observability matrix in order to identify the nonlinear multi-input, linear-in-the-states, multi-output system. We identify models (input/output characteristics) by applying this method for a number of sixteen flight conditions for which the Mach number varies from 0·85 to 1·30 and the altitudes vary from 5,000ft to 25,000ft. Very good results are obtained with a fit between the estimated and the measured signals and a correlation coefficient higher than 90%.

NOMENCLATURE

A,B,C,D	matrices describing the state-space model
AIL_L	left aileron position
AIL_R	right aileron position
Cov	covariance
F	projected noise matrix multiplied by the instrument
G	projected output matrix multiplied by the instrument
H	altitude or impulse response matrix
I	identity matrix
j	dummy index
M	Mach number
R	correlation coefficient
S	matrix of singular values
STB_L	left stabiliser position
STB_R	right stabiliser position
t, Δt	time, time step
T	projected state matrix multiplied by the instrument
TEF_L	left trailing-edge flap deflection
TEF_R	right trailing-edge flap deflection
u	system input vector
U	matrix of past or future inputs or matrix of singular vector
v	perturbation vector on the system outputs
V	future noise effect matrix or matrix of singular vector
Var	variance
Vec	operation which organises the parameters of a matrix into a column vector
$VERT_L$	left rudder position
$VERT_R$	right rudder position
w	perturbation vector on the system states
W	weight matrix
$WING_L$	left wing deflection
$WING_R$	right wing deflection
x	system state vector

Paper No. 3293. Manuscript received 16 April 2008, revised version received 23 October 2008 accepted 14 January 2009.

X	Matrix of past or future states
y	system output vector
$\hat{y}$	estimated output signal
z	discrete time shift operator
Δ	controllability matrix
η	Matrix of past output combinations used in the linear regression
θ	unknown parameters used in the linear regression
Γ	observability matrix
Π	projection operator
ϕ	phase
φ	columns of the instrument matrix
Φ	instrument matrix

Subscripts

f	future
h	number of past inputs used in the instrument matrix
k	k^{th} timestep prediction of noise effect (line *k*) on V matrix or k^{th} frequency
m	number of inputs
n	number of states or order of the system
N	length of data vector or approximation with a finite amount of data points
o	number of outputs
p	past
r	forward prediction horizon
s	number of lines of the instrument matrix
Weight	matrix with weight functions added

Superscripts

†	Moore-Penrose pseudo-inverse
T	transpose

Symbols

$\perp$	perpendicular projection
^	estimated value
∞	infinity

1.0 INTRODUCTION

The work presented in this paper uses flight flutter test data obtained from the active aeroelastic wing technology research program[1,2,3] at NASA Dryden Flight Research Center. Aeroelastic flutter involves the unfavourable interaction of aerodynamic, elastic, and inertia forces on structures to produce an unstable oscillation that often results in structural failure[4]. Thus, aeroelasticity plays a major role in the design of aircraft. Flight flutter test techniques are based on Von Schlippe's method: the structural excitation, the response measurement, and the data analysis for stability. The aircraft is piloted at several flight conditions by increasing the Mach number. Then, by analysing the data, it is possible to extrapolate the information in order to predict the aircraft stability at next flight condition.

The aim of the AAW Technology Flight Research Program, initiated in 1996, was to validate an aircraft concept in which a lighter, more flexible wing could be used to improve the F/A-18 roll performance by minimising the maneuver load on its wings. At high dynamic pressures, the AAW control surfaces can be used as tabs that are deflected into the air stream to produce wing twist which minimises the control surface motion needed for aircraft maneuvering. Increase of the control effectiveness at high velocities is therefore the main advantage of the active aeroelastic wing concept. The design of such an improved wing requires aeroservoelastic interaction studies between loads, flight vehicle unsteady aerodynamics, active controls and structural aeroelasticity.

In this paper, a model is presented which computes the structural deflections of the flexible F/A-18 Active Aeroelastic Wing following a given control input. The model is built using the subspace parameter estimation methods from flight flutter tests from Ljung N4SID method[5]. This subspace identification algorithm, a very efficient non-iterative system identification technique, is used for mathematical model identification. The next sections present a literature review on system identification methods, and in particular, on the subspace method used in aeroelasticity applications.

The autoregressive moving average method (ARMA) and neural networks were used by Sung *et al*[7] to identify the flutter behaviour of a transonic wing. Kukreja and Brenner[6] later used the nonlinear autoregressive moving average exogenous (NARMAX) model to study the flutter dynamics of a pitch-plunge system subjected to limit cycle oscillations. The dynamics of a flexible wing model has also been modelled by Silva *et al*[8] by use of the impulse response method and the Eigensystem Realisation Algorithm (ERA). An output-error minimisation method was performed based on a large flexible aircraft by Le Garrec *et al* [9].

The subspace method was already applied in many other fields such as fibre optics research[10]. In the aerospace field, the subspace method has been used to identify the effects of the aircraft's control surface motion on the rigid modes of an F/A-18 from flight flutter tests[11]. In this method, the ailerons were excited by use of Schroeder frequency sweeps. The structural accelerations of the aircraft were filtered using a wavelet transform and the aircraft responses were identified in both time and frequency domains. In the present study, the subspace identification method is used to identify the structural deflections of the F/A-18 Active Aeroelastic Wing aircraft's surfaces from flight flutter tests.

2.0 METHODOLOGY

The methodology part of this paper has three distinct sections:

A. Description of the Schroeder excitation inputs signals and data preprocessing

B. Description of the architecture of the state-space models

C. Description of the subspace system identification method.

2.1 Excitation inputs and data preprocessing

In order to obtain the recorded flight flutter tests data, the flight control computer (FCC) for the F/A-18 AAW aircraft was modified by adding a research flight control system (RFCS) to generate the Schroeder frequency sweep control inputs. The software used by the RFCS to control the actuators was called the on board excitation system (OBES). The Schroeder frequency sweep generated by the OBES is a sum of harmonics, equally spaced in the frequency domain. An example of the OBES control inputs time history is shown in Fig. 1.

The OBES Schroeder excitation signal is defined in Equation (1):

$$OBES(t) = \sum_{k=1}^{C} A_k \operatorname{Sin}\left(2\pi f_k t + \phi_k\right) \quad \ldots (1)$$

where f_k is the k^{th} measurement frequency, ϕ_k is the k^{th} phase and A_k is the k^{th} amplitude of the Schroeder signal. Details on the theory of Schroeder signals are given by Galvao *et al*[10]. The advantage to use Schroeder signal is that it minimises its peak-to-peak amplitude, which is very useful in aircraft inputs excitation. The OBES generated Schroeder signal is sent to the aircraft actuators to generate the F/A-18 control surfaces oscillations. For each flight test record, the excited control surfaces may be one of the following: differential aileron, collective aileron, collective stabiliser, differential stabiliser or rudders. The outputs of the mathematical model are the structural deflections of both wings

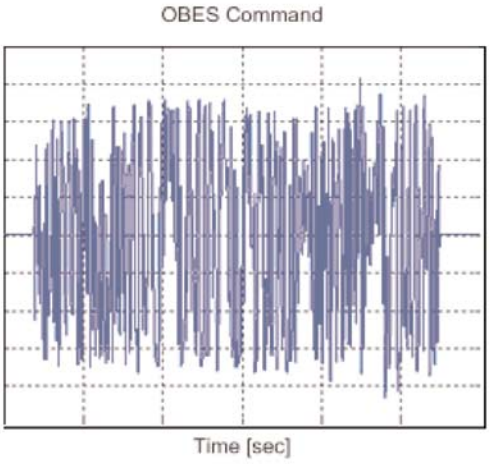

Figure 1. OBES control inputs versus time.

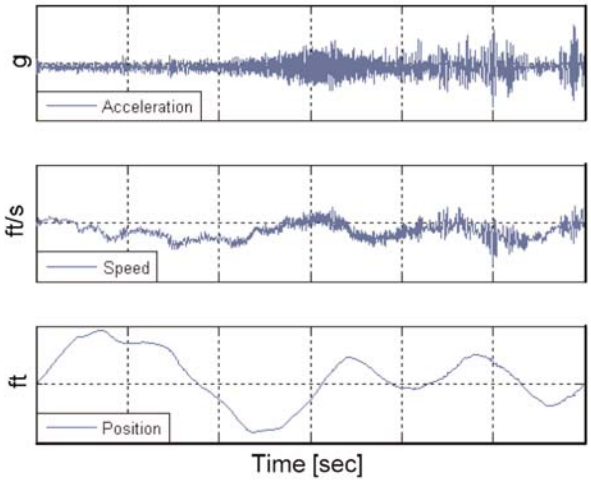

Figure 2. Left wing accelerations and their single and double integrations with time which give the velocity and the deflection in time.

and trailing-edge flaps. The tests were performed for a combination of Mach numbers from 0·85 to 1·20 and for altitudes from 5,000ft to 25,000ft. At each flight condition, characterised by an altitude and a Mach number, all the five different excitation inputs mentioned above were performed to generate different records with a time length of 30 seconds. In order to capture all the system dynamics when building the mathematical model, maneuvers corresponding to a given altitude and Mach number were concatenated to generate a single 150-sec time record.

In this paper, we use the measured structural accelerations provided by NASA Dryden. The measured accelerations on the structural surfaces are very noisy. We remove the noise in order to identify the F/A-18 AAW model by performing a double integration on the surface accelerations to obtain the surface deflections. The effect of integration on the accelerations is shown in Fig. 2, where velocity and position time histories are represented for the left wing surface over the 150-sec concatenated time interval. Only the structural surface deflection, velocity, and acceleration for the left wing are shown to illustrate the way in which integration operations remove the unwanted noise.

By observing Fig. 2, the double integration has produced smoother signals which can be easily estimated.

2.2 State-space model architecture description

The nonlinear multiple-input, multiple-output (MIMO) model representing the system is presented in Fig. 3.

The model linear inputs, represented by the upper left block of Fig. 3, are the left and right aileron positions AIL_L and AIL_R, the stabiliser positions STB_L and STB_R and the vertical tail $VERT_L$ and $VERT_R$ positions. These inputs are also combined with nonlinear inputs of second degree in order to improve the match between the model and the data. These nonlinear inputs are composed of polynomial combinations of the standard model inputs. The generation of these nonlinear inputs by multiplying the inputs together can also be thought of as a component of the overall mathematical model. Even though the identified state-space model is linear in the states, the overall model includes nonlinear terms. A similar approach of using nonlinear input is used in polynomial neural network models[12]. The outputs are the wing deflections $WING_L$ and $WING_R$ and the trailing-edge flap deflections TEF_L and TEF_R derived from the corresponding accelerometer measurements on the outer wing and the trailing-edge surfaces, respectively. The state-space matrices **A, B, C** and **D**, where columns of **B** and **D** account for the extra nonlinear inputs, are identified with the subspace method which will be explained in the following section[13].

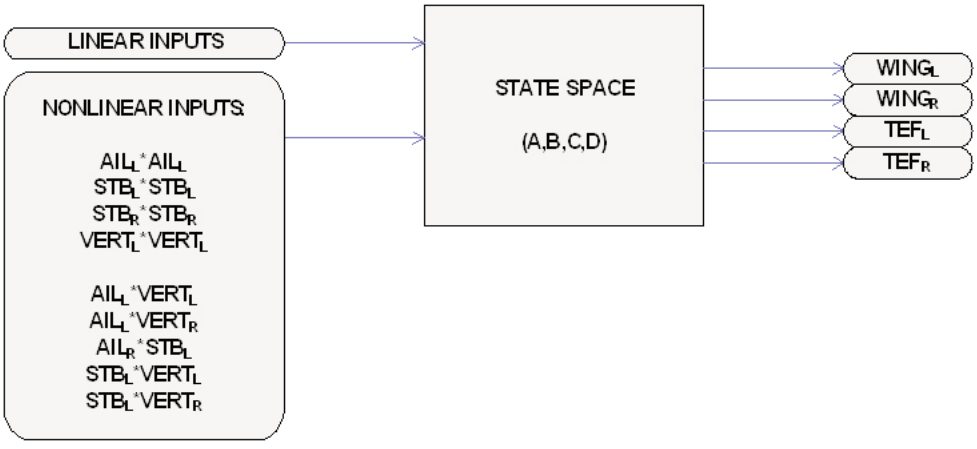

Figure 3. MIMO model with a nonlinear combination of the inputs.

3.2 Description of the subspace system identification algorithm used in this paper

3.21 The state space matrices

Generally, a discrete linear model is defined with the following Equations (2) and (3):

$$x\left(t+\Delta T\right)_{n\,x\,1} = \mathbf{A_{n\,x\,n}}\, x\left(t\right)_{n\,x\,1} + \mathbf{B_{n\,x\,m}}\, u\left(t\right)_{m\,x\,1} + w(t)_{n\,x\,1} \quad \ldots (2)$$

$$y\left(t\right)_{o\,x\,1} = \mathbf{C_{o\,x\,n}}\, x\left(t\right)_{n\,x\,1} + \mathbf{D_{o\,x\,m}} u\left(t\right)_{m\,x\,1} + v(t)_{o\,x\,1} \quad \ldots (3)$$

The **A, B, C** and **D** matrices terms are usually estimated by use of various parameter estimation methods. Most of these methods start with a set of initial guesses found from physical knowledge of the system. A minimisation algorithm is further used to reduce the error between the model output and the given flight test data. Unfortunately, with these methods, if the initial parameter guesses are far from their true values, the minimisation algorithm may converge towards a local minimum.

The main advantage of this subspace identification algorithm used in this paper is that it is non-iterative and does not require an initial guess [5] of the parameters inside the state-space matrices [**A, B, C, D**]. The accuracy of the resulting model usually compares to a model that would have been generated with an optimisation which would have converged near the global minimum. The only information required by the subspace method is the input and the output data vectors.

The subspace identification algorithm is implemented in the Matlab System Identification Toolbox. The manner in which the algorithm is implemented in Matlab® is given by Ljung[5]. The main concept of the subspace method is the definition of the system observability matrix Γr in the following Equation[4] from modern control theory, where r represents a forward prediction horizon[5]. This matrix can be obtained from the system inputs $u(t)$ and outputs $y(t)$ and its expression is the following:

$$\Gamma_r \overset{def}{=} \begin{bmatrix} C_{oxn} \\ CA_{oxn} \\ \ldots \\ CA^{r-1}{}_{oxn} \end{bmatrix}_{roxn} \quad \ldots (4)$$

Once this observability matrix Γr is known[5], the state space matrices [**A, B, C, D**] are obtained by use of the input and output vectors.

In this project, Ljung's algorithm is chosen to compute the subspace matrices of the system. Many investigations were done in the field of system identification such that vanOvershee and DeMoor who studied the theory, the implementation ans the applications of subspace identification algorithms for linear time-invariant finite –dimensional dynamical systems[14].

3.2.2 Selection of the mathematical model order

The subspace method explained above applies for a state-space model of any order. Recall that the order of a state-space model is defined by the rank of matrix **A** defined in Equation (2) and this order must be carefully selected in order to obtain an appropriate model. The order should be high enough to ensure that the model represents all the important system dynamics; however, choosing an order that is too high may lead to an over-fitting problem. Over fitting occurs when the model order is chosen too high for the length of data used in identification. The result is expressed by the identification of the unphysical system characteristics, producing a model that performs poorly for new data. A good approach for model order selection is therefore to insure that for a given order, the model performance is optimal for both the identification test data and another data set aside for the validation process. In this paper, there was no validation flight test data to evaluate the model's generality since the input frequency varied continuously across the time span and maneuvers were not repeated at the same flight condition. To solve this problem, robustness test data were generated by slightly perturbing the initial identification flight test data using a re-sampling technique. These robustness test data were used as validation data. The method used to generate these robustness test data is explained later. Different model orders are tried and for each order, the model performance on the identification flight test data and the robustness test data were evaluated. A plot is then given that shows the singular values of the Henkel matrices of the impulse response for different orders are graphed. The order can be selected such that the singular values are small for higher orders comparing with those of the lower orders. It was found that the optimal model order was eleven.

4.0 RESULTS

This section explains the way in which the nonlinear mathematical models obtained from the subspace system identification method are evaluated. The mathematical model is stated as nonlinear because even though state space model alone is linear, if its inputs have nonlinear components, the overall model (polynomial combination of the linear inputs + linear state-space model) is nonlinear. The accuracy of the mathematical model is demonstrated with four different criterions:

A. criterions used to evaluate the model
B. the match between the model output and the output from the flight test data expressed by qualitative tests for one flight condition.
C. summary of results obtained for all flight conditions.
D. graphical representation of correlations between the model vs data.

The results section is divided into three parts: the first part explains the criterion used to evaluate the model. These criterions are the correlation and the fit coefficients, and the robustness test. The second part shows graphically the match between the model outputs and the input data for a given flight condition. The third part summarises the results for all flight conditions by use of the average correlation coefficients and fit coefficients. The last part shows graphically the worst results.

4.1 Criterion used to evaluate the model

4.1.1 Correlation coefficient

The first method used to validate the model is the correlation coefficient. The correlation coefficient R equal to one ($R = 1$) denotes perfect linear dependency (no scatter) between the measured and the calculated or estimated outputs. A correlation coefficient equal to minus one ($R = -1$) denotes inverse linear dependency between the measured and the estimated outputs. A correlation coefficient of zero ($R = 0$) denotes the linear independency between the measured and the estimated outputs. A good correlation coefficient between the output from the model and the flight test data indicates that there are no unusual error between the model and the data. However, it does not give enough information about the overall goodness of the fit. A better measure of the model performance can be obtained by the second method: the fit coefficient.

4.1.2 Fit coefficient

The fit coefficient is defined as 100% multiplied by the ratio between the L_2-norm of the error between the data and the model over the L_2-norm of the error between the data and its mean value. The fit coefficient is expressed by Equation (5):

$$FIT = 100\left(1 - \sqrt{\frac{\sum_{1}^{n}(y-\hat{y})^2}{\sum_{1}^{n}(y-mean(y))^2}}\right) \quad \ldots (5)$$

The main advantage of using the fit coefficient is that it takes into account the data variation about its mean in order to evaluate the model quality. For example, even if a model has an output very close to the data output, it will have a poor fit coefficient if there are much more small oscillations in the data than in the model.

4.1.3 Robustness test: model capability

Normally, the best manner to test the performance of a model i.e. to validate the identified model would be its use in a simulation with a set of input data which was not used in the parameter identification process. The resulting model output is then compared to the flight test data outputs corresponding. This comparison can be done by using the correlation and fit coefficients and this test is called cross-validation. Unfortunately, in this paper, it was not possible to set data aside for the validation because there was only one set of data records available for each given input excitation, altitude or Mach number. For this reason, we decided to evaluate the robustness of our estimated model by considering the model's output resulting from a simulation with slightly perturbed input signals. The purpose of this test was to evaluate the effect on the model's output of negligible input signals perturbations. If the model is not sensitive to very small perturbation of its inputs, it indicates that the model is robust. The difference between a perturbed input signal and the initial input signal is illustrated in Fig. 4.

The perturbed input signal shown in Fig. 4 was generated by performing the following operations: (1) first, resample the signal by keeping only one point for a given number b of points and then (2), reconstruct the signal from these points by performing interpolations in order to obtain the initial sampling rate.

This procedure is illustrated in Fig. 5 where Δt is the sampling rate over the 150-sec concatenated time interval.

This is equivalent to adding many small perturbations to the inputs signals in order to measure the sensitivity of the model to these perturbations. Thus, if the model is robust, it must react well to small perturbations of the input signals. This means that there is neither divergence nor oscillations on the output signals and the output fit parameters must be similar to the fit of the signal used in the identification.

The robustness test was used to select the most appropriate nonlinear inputs to be used and to build the models. These modified data sets were also used to select the most appropriate model order. Recall from Fig. 3 that the model's inputs are the different control surfaces deflections and nonlinear combinations of these deflections. The use of a high number of nonlinear inputs may cause the model to over-fit the data. When this situation occurs, there is a small model error compared to the data set used to build it, but the model performs poorly on these new data sets. Nonlinear inputs were added from the simplest to more complexes, and only kept if the nonlinear input improved the fits based on correlation and fit coefficients.

Since we do not have a separate data set to use in the cross-validation, we decided to use the modified input data for the robustness test above described as added nonlinear input would likely cause an over-fitting problem. We chose to add only the nonlinear inputs which improved the model performance on both the original data and the modified data used in the robustness test. In each case, the model performance was calculated in term of correlation and fit coefficients.

The following section will demonstrate qualitatively the model performance by showing the time history of the model output with respect to the time history of the flight test data for a given flight condition. This shows the mean results of the fit and correlation coefficients for all flight conditions considered in this paper.

4.2 Qualitative results for one flight condition

The following figure shows the results obtained for the model identification by use of the subspace method for both sets of data used in the

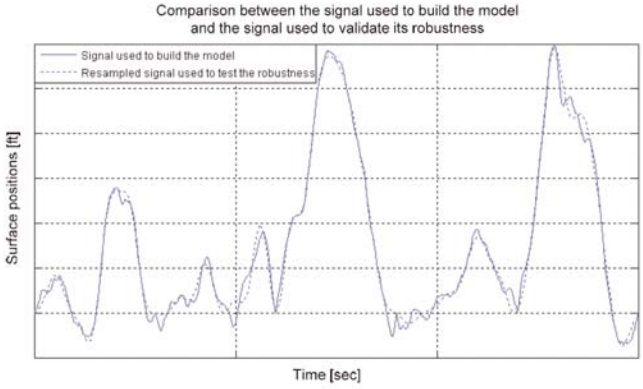

Figure 4. Perturbed signal used for the robustness test.

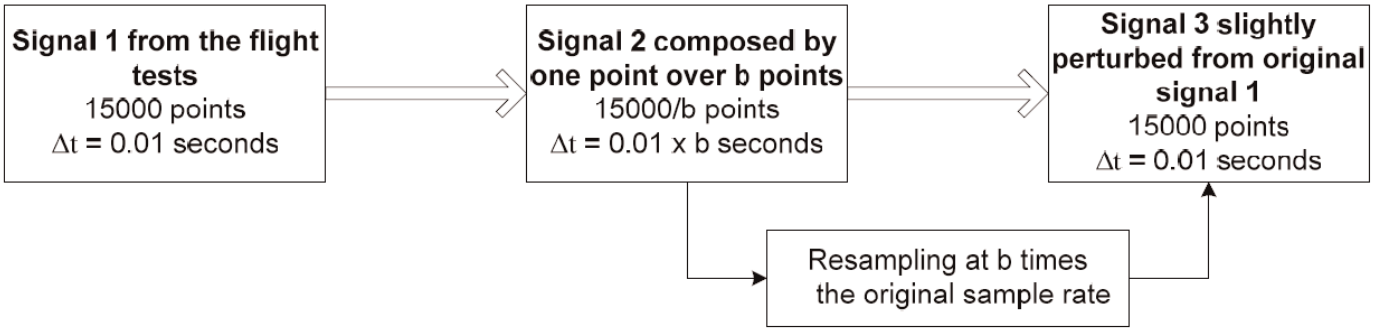

Figure 5. Input data modification for the robustness test.

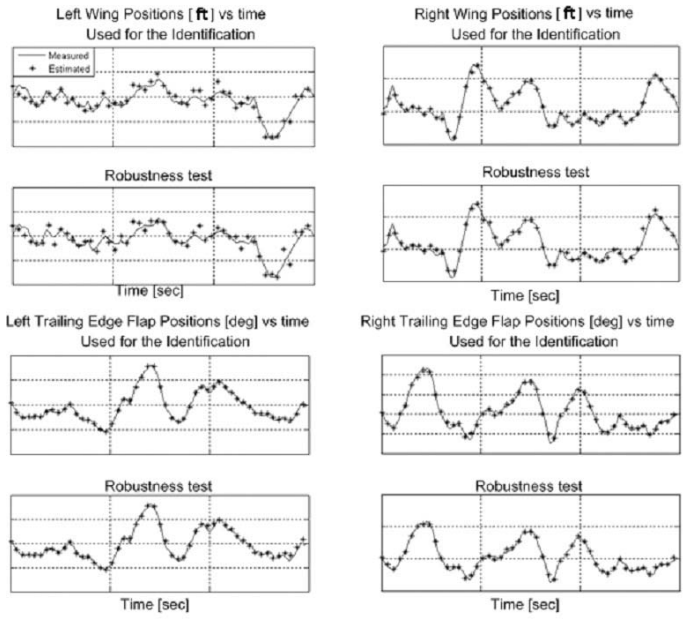

Figure 6. MIMO model identification and robustness test for M = 0·85 and *H* = 5,000ft.

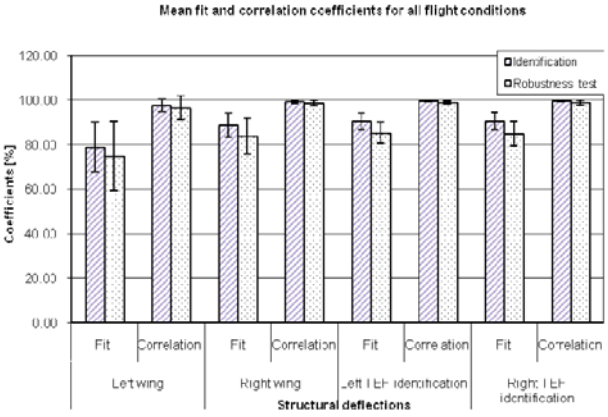

Figure 7. Mean value and standard deviation of the fit and correlation coefficients for every flight conditions.

Table 1
Correlation coefficients for the initial signals and resampled robustness test signals for M = 0·85 and H = 5,000ft

	$WING_L$	$WING_R$	TEF_L	TEF_R
Identification data, %	92·09	99·28	99·61	99·37
Modified Data for Robustness test %	90·88	98·23	99·26	99·18

Table 2
Fit coefficients for the initial signals and resampled robustness test signals

	$WING_L$	$WING_R$	TEF_L	TEF_R
Identification data, %	57·56	87·11	91·13	88·73
Modified Data for Robustness test %	54·04	80·66	87·33	87·17

identification and in the robustness test. These results are for a Mach number of 0·85 and an altitude of 5,000ft. In Fig. 6, the solid line represents the measured output from the flight test data and the stars represent the model output over the 150-sec concatenated time interval.

From a visual inspection, is clear that each model outputs match very well the flight test data for both the original data and the data modified for the robustness test for the aircraft different surfaces. Table 1 shows the correlation coefficients between the estimated and the measured outputs.

It can be observed that the correlation coefficients, for the flight conditions M = 0·85 and H = 5,000ft are very good, as they are all higher than 90%. Most of the fit coefficient results are also very good except for the left wing deflection which has a fit coefficient of 57·56% for the data used in the identification and a fit of 54·04% on the data used for the robustness test. Even though these fit coefficients are low, the left wing deflection time history graphs for estimated and measured results are still close, as seen on Fig. 8. Another observation which can be made is that there is not a high difference between the model accuracy on the data used in the identification with respect to the modified data for the robustness test.

4.3 Results summary for all flight conditions

The results above shown in Tables 1 and 2 are given for a single flight condition characterised by a Mach number of 0·85 and an altitude of 5,000ft. In this paper, F/A-18 aircraft model with different set of parameters were identified for a number of 16 different combinations of Mach numbers and altitudes, see Table 3.

The mean value and the standard deviation of the fit and correlation coefficients were computed for all these flight conditions and the results for each aircraft surface are illustrated in Fig. 7.

In Fig. 7, the bar represents the mean value of the fit or correlation coefficients for both the data used in the identification and the data modified for the robustness test. The following observations can be made from this figure:

a) The correlation coefficient between the model output and the flight test data output is always near 100% and re-sampling the data for the robustness test has a very small effect on the correlation coefficient.

b) The fit coefficient is higher than 80% for every structural surface except the left wing which is slightly lower and modifying the data for the robustness test also has a small effect.

These good results for the correlation and the fit coefficients indicate that the model is accurate. There is a very small degradation of the fit and correlation coefficients when the inputs resampled inputs for the robustness test are used, which indicates that the model is robust and does not over-fit the data. Please note that the model is slightly less accurate in the left wing deflection prediction. Table 4 below shows, as an example, the fit and correlation coefficients for the left wing deflection calculated by the model and the deflection from flight flutter test data for all flight conditions defined in Table 3.

From Table 4, is seen that the three worst results are given for flight conditions 1, 4 and 6. The time histories of these worst results are shown in the next section.

4.4 Worst results

From the table 4 above, we notice that three flight conditions do not well satisfy the previous conclusions and they are: M = 0·85, *H* = 5,000ft; M = 0·90, *H* = 5,000ft and M = 0·90, *H* = 15,000ft. The estimated and measured outputs related to the worst flight conditions cases are visually shown in Fig. 8 over the 150sec concatenated time interval.

For each flight condition represented in Fig. 8, the left wing deflection from the model is shown with respect to the deflection

Table 3
Summary of the different flight conditions used in this paper in terms of altitudes and Mach numbers

Flight Condition	**1**	**2**	**3**	**4**	**5**	**6**	**7**	**8**	**9**	**10**	**11**	**12**	**13**	**14**	**15**	**16**
Mach Number	0·85	0·85	0·85	0·9	0·9	0·9	1·1	1·1	1·1	1·1	1·2	1·2	1·2	1·2	1·3	1·3
Altitude 10^3 feet	5	10	15	5	10	15	10	15	20	25	10	15	20	25	20	25

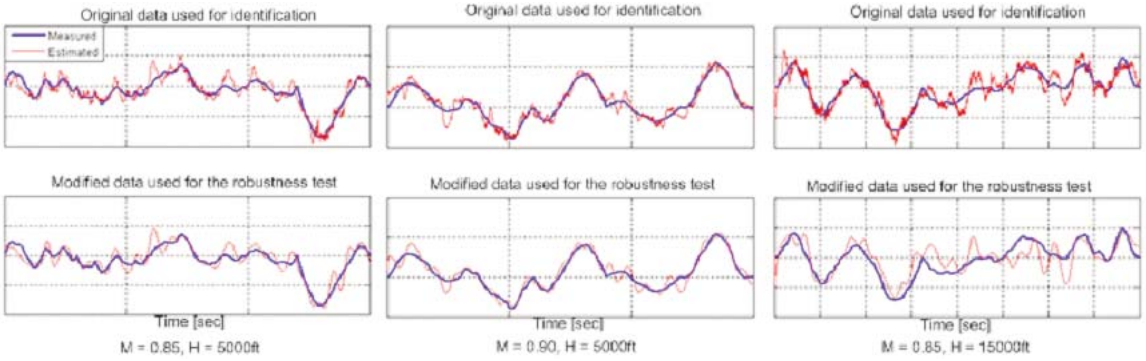

Figure 8. Three worst cases for the left wing deflections (ft) outputs.

Table 4
Fit and Correlation coefficients for the left wing deflection for all flight conditions

Flight Condition	**1**	**2**	**3**	**4**	**5**	**6**	**7**	**8**
Fit	57·56	76·41	80·56	69·36	73·63	54·12	87·21	81·04
Correlation	92·09	97·45	98·64	95·39	96·97	91·54	99·23	98·29
Flight Condition	**9**	**10**	**11**	**12**	**13**	**14**	**15**	**16**
Fit	87·89	86·00	93·92	80·77	89·81	86·12	84·35	77·49
Correlation	99·27	99·13	99·82	98·44	99·53	99·11	98·80	98·33

from the flight test data. In each case, the deflection model output was found by use of the inputs from the original data and the modified input from the robustness test. We observe that there exist oscillations of the identified signal in Fig. 8. Yet, we can say that the trends of the estimated signals follow the measured signals. The oscillations do not generate instabilities or divergences of the output signals. Therefore, we noted that the worst results affect only the first output of the system which is the left wing position (WINGL). For the robustness test signals there are also oscillations but they are less pronounced, and the robustness test signals have the same trends as the measured signals.

5.0 CONCLUSIONS

- A state space nonlinear multi-inputs, multi-output model was used in this study to estimate structural surface deflections given by the F/A-18 control inputs for sixteen flight conditions characterised by different Mach numbers and altitudes. The subspace identification method was used for the model identification from flight flutter tests.
- Two methods were used to calculate the differences between data and model-identified outputs: the correlation coefficients, and the fit coefficient. Except for the three worst left wing cases, good results were found for all flight conditions and were characterised by correlation coefficients higher than 96% and fit coefficients higher than 73%. Then, resampled signals were used to test the robustness of the identified model. The same eleventh order model from the correlation and fit coefficients was found.
- Another method to check the model capability and so its validation would be to compare estimated signals from other sources not used to identify the model. The robustness test and the validation on complementary data would represent a strong validation method.
- The advantage of the subspace identification method applied to our model is its small computing time and also the estimation of a very good model only from flight test inputs and outputs. The estimated nonlinear-input, linear-in-the-states model was found to be robust by application of the re-sampling technique. Hence, this subspace approach method seems very convenient for model identification from flight flutter tests.

ACKNOWLEDGMENTS

We would like to thank to Mr Marty Brenner from NASA Dryden Flight Research Center for his collaboration on this work. Financial support for the work related to this paper was given by the Natural Sciences and Engineering Research Council of Canada NSERC and by the Ministère du Développement économique, de l'Innovation et de l'Exportation MDEII.

REFERENCES

1. VORACEK, D., PENDLETON, E., REICHENBACK, E., GRIFFIN, K. and WELCH, L. The active aeroelastic wing phase I Flight Research through January 2003, NASA TM-2003-210741, April 2003.
2. LEE, D., BALDELLI, D., LINDSLEY, N. and BRENNER, M. Static aeroelastic and open-loop aeroservoelastic analyses for the F/A-18 AAW Aircraft, AIAA Paper 2007-213548, April 2007.
3. PENDLETON, E., FLICK, P., PAUL, D., VORACEK, D., REICHENBACH, E. and GRIFFIN, K. The X-53 A summary of the active aeroelastic wing flight research program, AIAA Paper 2007-185548, April 2007.
4. KEHOE, M.W. A historical overview of flight flutter testing, NASA Technical Memorandum 4720, 1995.
5. LJUNG , L. *System Identification Theory for the User*, 2nd (Ed), Prentice Hall, 1999, pp 340-351.
6. SUNG WON, K, TSAI H., M., SADEGHI, M. and LIU, F. Nonlinear impulse methods for aeroelastic simulations, AIAA Paper 2005-4845, June 2005, pp 1-19.
7. KUKREJA, S.L. and BRENNER, M. Nonlinear aeroelastic system identification with application to experimental data, *AIAA J Guidance*, *Control and Dynamics*, 2006, **29**, (2).
8. SILVA, W.A., VARTIO, E., SHIMKO, A., SEGUNDO ,EI, KVATERNIK, R. G., EURE, K.W. and SCOTT, R. Development of aeroservoelastic analytical models and gust Load alleviation control laws of a sensorcraft wind-tunnel model using measured data, AIAA Paper 2006-1935, May 2006.
9. LE GARREC, C., HUMBERT, M., BUCHARLES, A. and VACHER, P. In flight aeroelastic model identification and tuning of a flight control system on a large civil aircraft, CEAS International Forum on Aeroelasticity and Structural Dynamics, Madrid, Spain, June 2001.
10. GALVAO, R.K.H., HADJILOUCAS, S., BECERRA, V.M. and BOWEN, J.W. Subspace system identification framework for the analysis of multimoded propagation of THz-transient signals, Institute of Physics Publishing, *Measurement Science and Technology*, 2005, **16**, pp 1037-1053.
11. BRENNER, M. and FERON, E. Wavelet analysis of F/A-18 aeroelastic and aeroservoelastic flight test data, AIAA paper A97-24112 05-09, April 1997.
12. LUIS, S.B., DA SILVA, BOSE, B.K., JOAO and PINTO O.P., Recurrent Neural Networks based implementation of programmable cascaded low pass filter used in stator flux synthesis of vector controlled induction motor drive, IEEE Transactions on Industrial Electronics, **46**, (3), June 1999.
13. LENNART, L. System Identification Toolbox for use with Matlab®, User Guide Version 6, The Mathworks Inc, 2006.
14. VANOVERSHEE, P. and DEMOOR, B. *Subspace Identification of Linear Systems: Theory, Implementation, Applications*, Kluwer Academic Publishers, 1996.